Int. J. Simul. Multidisci. Des. Optim. **15**, 8 (2024)
© A. Zereg et al., Published by EDP Sciences, 2024
https://doi.org/10.1051/smdo/2023024

IJSMDO
Available online at:
https://www.ijsmdo.org

RESEARCH ARTICLE

OPEN ACCESS

Performance enhancement of Savonius wind turbine through partially deformable blades

Alaeddine Zereg[1], Mohamed Taher Bouzaher[2], Mounir Aksas[3], and Nadhir Lebaal[4,*]

[1] LPEA, University of Batna 1, Batna, 05000 Algeria
[2] Scientific and Technical Research Centre for Arid Areas (CRSTRA), Biskra, 07000 Algeria
[3] LEREESI, Higher National School of Renewable Energy, Environment & Sustainable Development, Batna, Algeria
[4] ICB UMR 6303, CNRS, University of Bourgogne Franche-Comté, UTBM, 90010 Belfort, France

Received: 9 October 2023 / Accepted: 9 December 2023

Abstract. In this study, we employ partially deformable blades to elevate the performance of Savonius wind turbines. The Bucket is constructed with rigid components equipped with a guidance system, resulting in continuous changes in its shape during turbine rotation. As the trailing edge of the advancing blade expands, it creates an active slot, effectively correcting the Bucket's pressure distribution and enhancing the positive torque generated by the turbine. We employ a two-dimensional (2D) numerical model, implemented using the commercial software ANSYS-Fluent 23.0, with the governing motion equation executed through a user-defined function (UDF). This investigation explores the mechanism of performance enhancement by varying expansion amplitudes Our results, obtained at a Tip-speed ratio (TSR) of 1, reveal that when the amplitude of deformation exceeds one-quarter of the Bucket radius, the partially deformable blade outperforms the rigid blade, leading to a remarkable 32% improvement in the torque coefficient. These findings signify a promising path toward enhancing Savonius turbine efficiency.

Keywords: Savonius turbine / deformable blade / wind turbine efficiency / harvesting wind energy

1 Introduction

Over the past decade, energy consumption has sharply increased, driven by population growth and technological advancements [1]. Meeting this rising energy demand with sustainable and limitless sources has become crucial for economic growth. To address this challenge, various systems for harnessing energy from renewable sources have been developed or enhanced [2]. Two natural resources that can be harnessed for energy are tides and wind, which can be conventionally captured using rotating turbines [3]. These turbines are categorized into horizontal turbines, with axes of rotation parallel to the incoming flow, and vertical turbines, with axes perpendicular to the flow. Among vertical turbines, there are Savonius turbines (drag-based) and Darrieus turbines (lift-based), along with some using combined lift and drag forces [4]. Numerous studies have aimed to improve the performance of Savonius turbines [5]. Most of these efforts have focused on modifying blade shapes, and thickness, or using baffles to alter their interaction with the incoming flow [6]. For example, placing a circular cylinder upstream of the returning blade can enhance performance by 12.2% at a specific tip speed ratio [7]. Additionally,, using obstacles like curved circular plates in front of the blades has increased turbine performance by up to 19% [8]. Deformable blades have also been explored to reduce returning blade drag. Some researchers have proposed rigidly deformable blades that open when advancing and close when returning, resulting in a 25.9% improvement in performance [9]. Self-expandable blades that passively expand relative to the turbine angle have demonstrated the potential to increase the torque coefficient by 90.6% [10]. Studies involving elliptical and radii deformable blades have shown promise for novel energy extraction methods [11,12]. Vertical strips have been proposed to control the negative effects of high wind speed, effectively turning rigid blades into blades with numerous openings [13]. Hinged blades with a guiding system have improved efficiency by 52% [14]. Flexibility in turbine blades has also received attention. Turbines with elastic blades that deform due to fluid loads have shown a remarkable 90% improvement compared to rigid turbines [15]. Tidal turbines with flexible blades, which open up in response to incident flow, have indicated the potential for performance enhancements under specific flow conditions [16].

* e-mail: nadhir.lebaal@utbm.fr

Table 1. Benchmarking table for recent researches on the Savonius turbine.

References	Blades type	Method and analysis	Key findings
This work	Partially deformable blades	Numerical analysis (CFD)	A remarkable improvement in torque coefficient with 32%.
Dominicus et al. [17]	Slotted Blades	Experimental investigation	The turbine with a 10% overlap ratio showed the best performance with an improvement of 28% in power coefficient.
Fatahian et al. [18]	Blades with deflector	Numerical analysis (CFD)	By adding a deflector, the power coefficient enhanced dramatically up to 24.2%.
Kaya et al. [19]	Elliptical blades	Numerical analysis (CFD)	The elliptical design model produced a maximum power coefficient that was over 30 greater than the based one.
Priyadumkol et al. [20]	Modified Blade	Experimental investigation	A higher power coefficient compared to the conventional rotor by 6.67% and 18.75% for a Reynolds number of 136640 and 156160, respectively.
Manganhar et al. [21]	Blades with Guiding rotor house	Numerical analysis (CFD)	The implementation of GRH led to an enhancement in the rotor's power coefficient of roughly 27%

Table 1 compares the findings of this research with several other key studies in the area of flow control technology that have been previously published.

In summary, research and development efforts have explored various techniques, including blade modification, obstacle placement, and deformable blades, to enhance the performance of Savonius turbines and other vertical turbine designs, offering promising solutions to address energy challenges and promote sustainability.

This work suggests a new Savonius vertical axis wind turbine model with partially deformable blades. The present model has so far not been proposed by other authors. The effect of deformation amplitude and the length of expandable parts have been investigated. The results indicate that at a Tip-speed ratio (TSR) of 1, when the amplitude of deformation exceeds one-quarter of the Bucket radius, the performance of the partially deformable blade is significantly superior to that of the rigid blade. Specifically, the torque coefficient exhibits an impressive improvement of approximately 32%. The proposed investigation has the potential to significantly enhance the performance of Savonius wind turbines, opening the path to higher efficiency.

2 Description of the proposed model

Figure 1 depicts the suggested model, which is a Savonius vertical axis wind turbine with partially deformable blades. Each blade has two parts: a rigid part connected to the turbine axis, which performs a pure rotation motion, and a radii deformable part that has a combined rotation/deformation motion (see Figs. 2a and 2b). The Bucket form

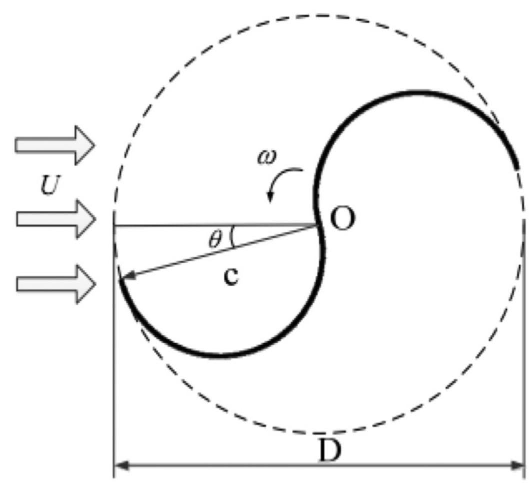

Fig. 1. Savonius turbine with rigid blade.

changes continuously during the turbine rotation. When the trailing edge of the advancing blade expands, an active slot is created. This slot achieves its maximum amplitude in every quarter of the cycle and is closed with a half-turbine rotation. The initial diameter of the turbine before deformation is 1 m (radius = 0.5 m). The swept area A_S remains the same because the expansion and the contraction have the same amplitude. So, the power available for extraction can be expressed as:

$$P_w = \frac{1}{2}\rho A_S U_\infty^3. \quad (1)$$

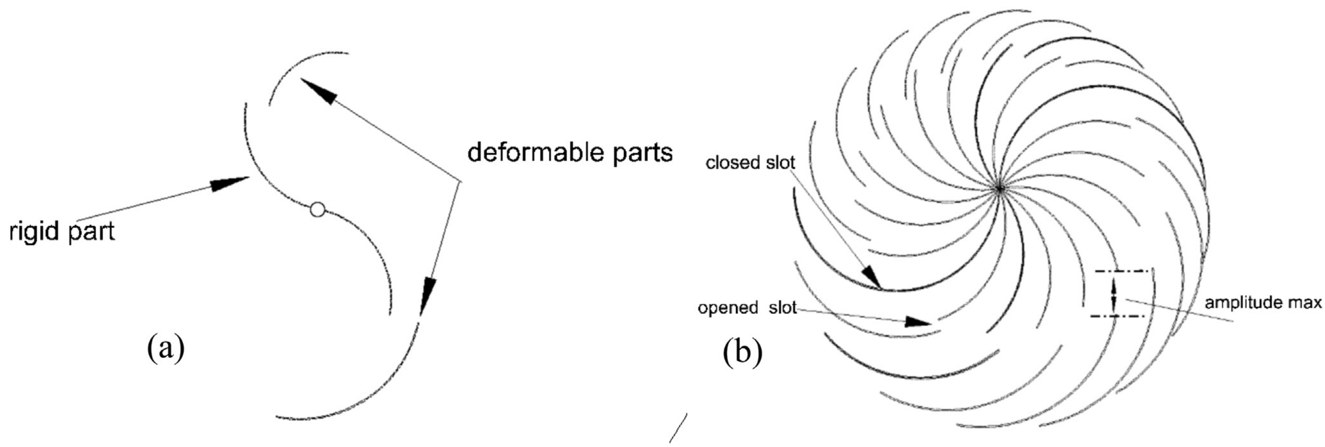

Fig. 2. (a) Savonius turbine with partially deformable blades (b) deformation over time.

Table 2. Turbine geometry parameters.

Parameter	Value
Rotorradius (R)	0.5 m
Height (H)	1 m
A_s	1 m^2
Blade Thickness (s)	0.0024 m
Bucketradius (R_1)	0.25 m

The power coefficient can be defined as the ratio between the energy extracted by the turbine and the total obtainable energy [17–22]:

$$C_P = \frac{P_m}{P_w} = \frac{P_m}{\frac{1}{2}\rho A_S U_\infty^3}. \quad (2)$$

The torque coefficient C_t is defined as:

$$C_t = \frac{T}{\frac{1}{2}\rho A_S U_\infty^2 R}. \quad (3)$$

In this examination, the frequency of expansion matches that of rotation, and the different amplitude of expansion ranged from $A = 0.125\,R_1$ to $A = 0.5R_1$ are examined. where R_1 represents the bucket radius. The rotor geometrical parameters are summarized in Table 2

3 Numerical method

3.1 Turbulence model

Practically, the flow around rotating machinery involves flow separation, swirl effect, and adverse pressure gradient. Thus, to predict correctly such flow behavior, the turbulence model must be selected judiciously. The RNG k–ε model was used in this work. The RNG k–ε and SST k-w models are among the most frequently used models in CFD modeling of Savonius turbine [23–25]. The near-wall treatment was employed. The first grid cell requires being at about **y+ ≈1**. A deformable computational mesh is displayed in Figure 3. The external domain dimensions are selected to ensure that flow is fully developed.

3.2 Motion equation

The 2D numerical simulation is approved using ANSYS FLUENT v18.1. The

The deformable turbine equation is executed within the DEFINE GRID MOTION macro. These equations are given as:

$$x = x_{old} \cdot A \sin(\omega_1 t + \varphi), \quad (4)$$

$$y = y_{old} \cdot A \sin(\omega_1 t + \varphi). \quad (5)$$

where y_{old} and x_{old} represent the blade position along x and y-axis in the previous time step. The angular velocity $\omega_1 = 2\pi f_1$ where f_1 is the deformation frequency.

3.3 Boundary conditions

Boundary conditions (BC) are defined in detail in Table 3. The BC corresponds to the 2D computational domain presented in Figure 3.

The tip speed ratio (TSR) changes from 0.4 to 1.2 and the amplitude of expansion from 0.125 R_1 to 0.5 R_1, where R_1 is the turbine bucket radius $(R/2)$.

The time steps (Δt) are selected to be reliable with 0.5 degrees of rotation every one Δt [21–26]. The time steps are linked to the angular velocity ω and accordingly to the tip speed ratio by equation (6).

$$\Delta t \frac{2\pi}{\omega} \cdot \frac{1}{360/0.5}. \quad (6)$$

The used time steps are listed in Table 4.

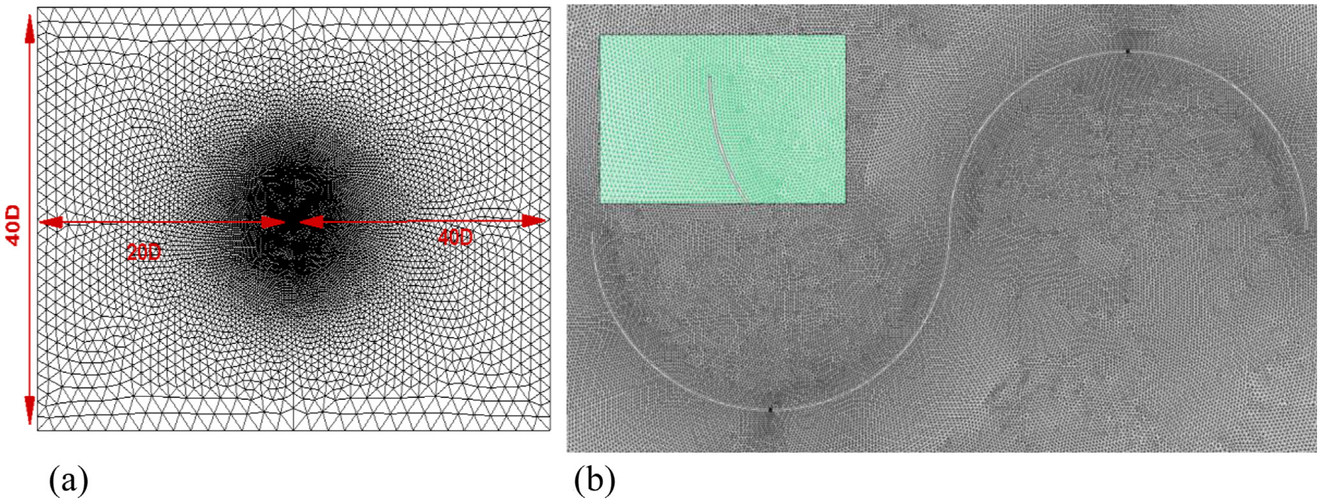

Fig. 3. (a) Deformable computational mesh (b) External domain dimensions (dimensions do not correspond to the scale).

Table 3. Boundary conditions.

Boundary	Parameter	Value	Note
Inlet	Constant velocity	7 m/s	Inlet turbulent viscosity = 0.001 m^2/s
Outlet	Gauge pressure	0 Pa	Outlet turbulent viscosity = 0.001 m^2/s
Sides	Symmetry	/	/
Blades	Wall	/	No slip wall condition

Table 4. Time steps versus tip speed ratio.

TSR[−]	ω[rad/s]	Δ t[s]
0.4	5.6	$1.5.10^{-3}$
0.7	9.8	$8.9.10^{-4}$
1	14	$6.2.10^{-4}$

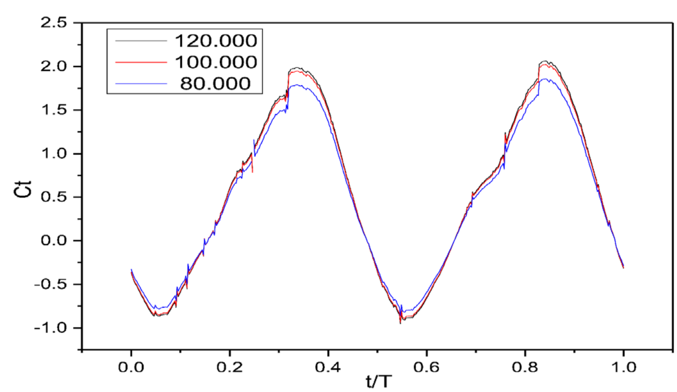

Fig. 4. Effect of grid densities on the torque coefficients for one period.

4 Results

4.1 Grid independence test and model validation

The reliability of the mesh model is confirmed by testing three grids with different densities. Figure 4. Shows the results of the computational test. It can be seen that when the mesh size exceeds 100.000 cells, plots overlap with each other. Reasonably, the grid quantity test is proved. To reduce computation cost without sacrificing accuracy, the mesh size of 100.000 cells (420 nodes on the turbine blade) is used for all cases. The grid specifications of the present mesh are listed in Table 5:

The experimental data from [27] are used as a benchmark to validate the present model. Figure 5 depicts a comparison between the experimental and CFD torque and power coefficients. It can be seen that the results are very close which reveals the validity of the numerical method.

4.2 Comparative analysis between deformable and conventional turbine

Figure 6 depicts the individual torque coefficient for rigid and deformable blade case A = 0.375 R_1, TSR = 1. Todescribe the flow behavior sufficiently during the turbine rotation, pressure contour for different instants is provided. Results reveal that the hinged or deformable turbine tends to reduce the torque fluctuation thus; the torque peaks of the conventional turbine are greater than that of the deformable blade this is attributed to the fact that at the onset of the deformation, a slot (void) is formed between

Table 5. Grid specifications of the present mesh.

Mesh density	Coarse	Medium	Fine
Total number of cells	80,000	100,000	120,000
Number of cells in the near wake zone	50,000	60,000	70,000
Number of cells in the far wake zone	30,000	40,000	50,000
First layer thickness (mm)	0.5	0.1	0.05
Number of nodes on the turbine blade	260	420	630
Average y+	2.1	0.4	0.3

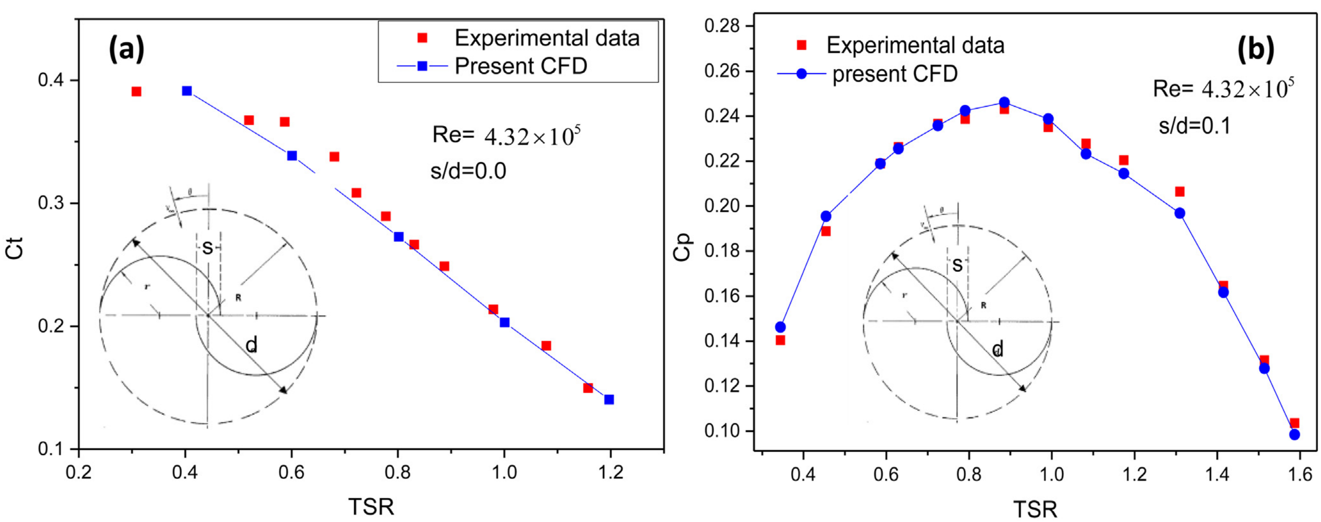

Fig. 5. CFD model compared to experiment data [27] (a) torque coefficient (b) power coefficient.

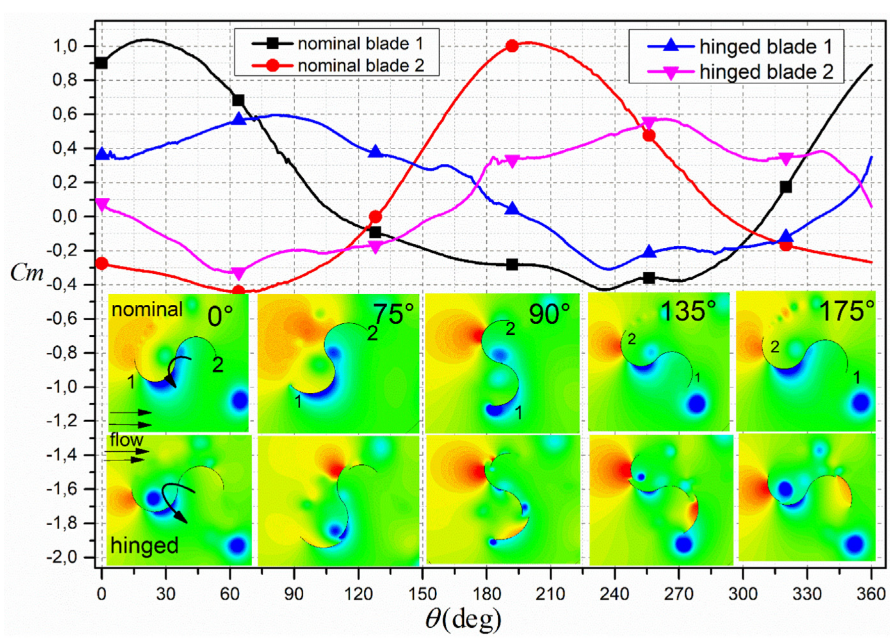

Fig. 6. Comparison of the individual torque coefficient for rigid and deformable blade case A = 0.375 R_1 and Pressure contour for different instants for rigid and expandable blade.

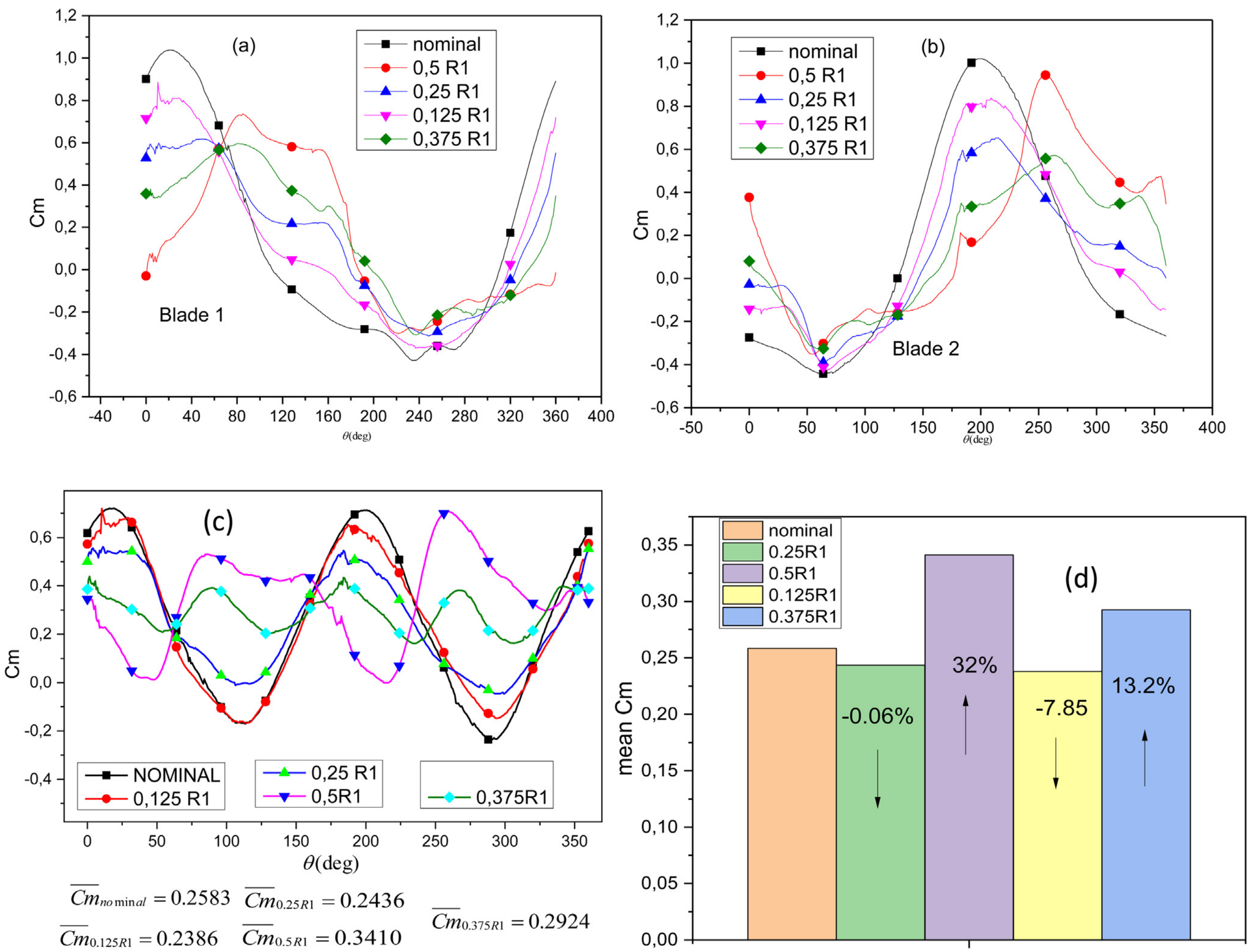

Fig. 7. Effect of expansion amplitude on the instantaneous torque coefficient of (a) blade A (b) blade B and (c) the total torque coefficient at TSR = 1.

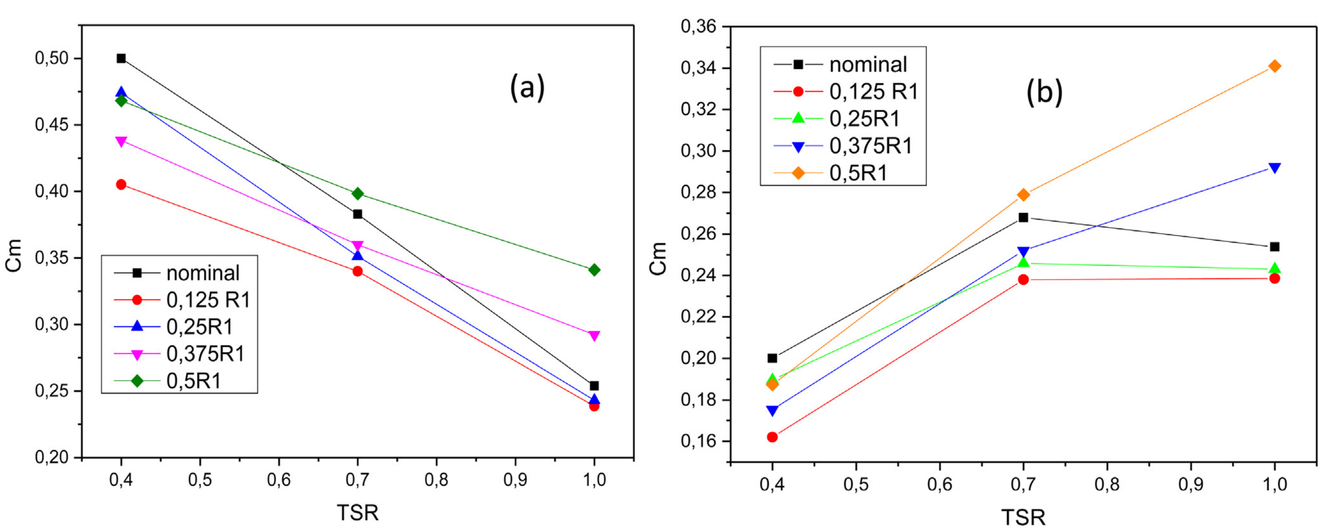

Fig. 8. Effect of expansion amplitude on (a) Average torque coefficient CT (b) Average Power coefficient CP.

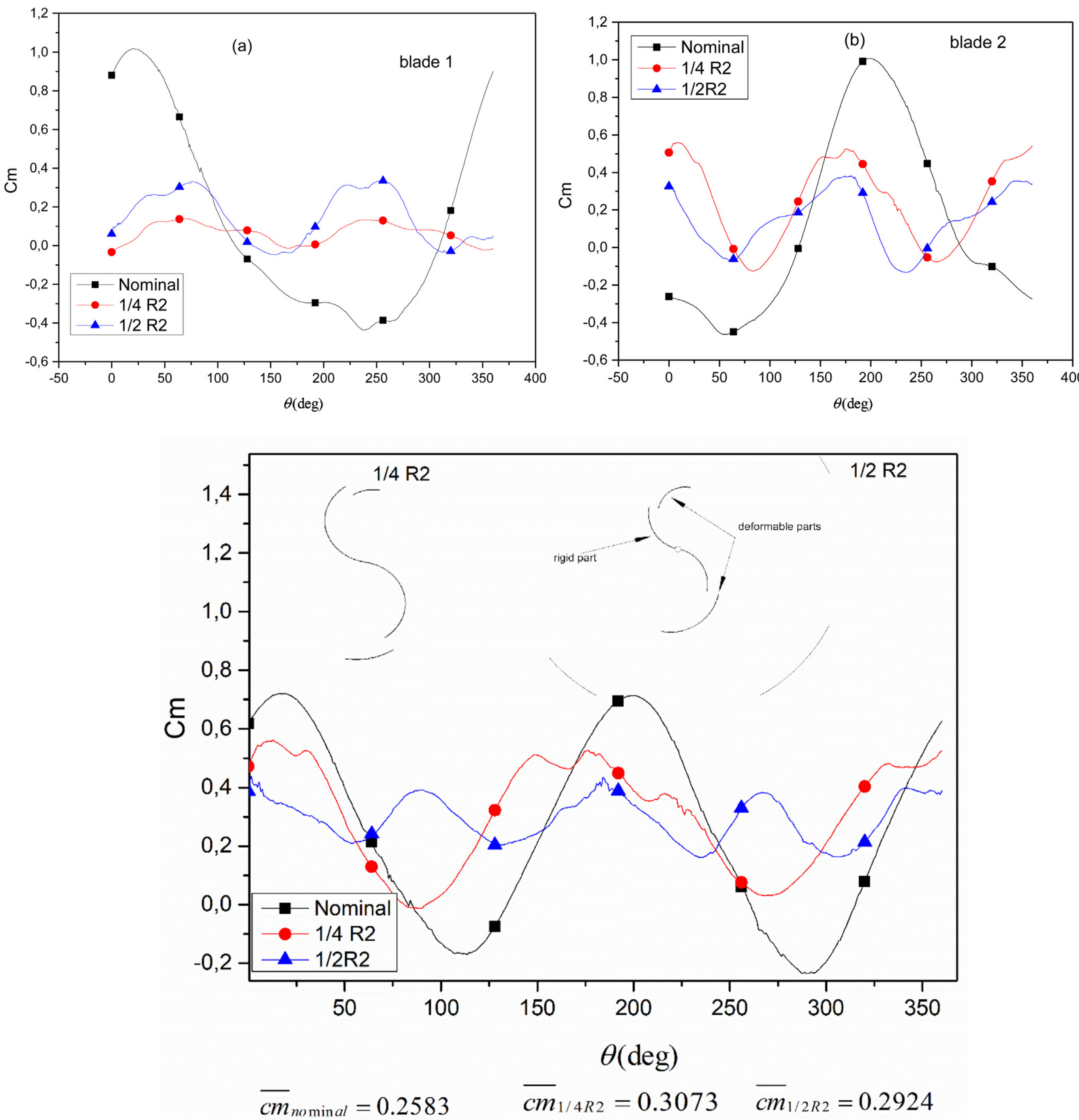

Fig. 9. Effect of deformable part length on the instantaneous torque coefficient of (a) blade A (b) blade B and (c) the total torque coefficient for A = 0.375 R_1 at TSR = 1.

the blade rigid and deformable parts, which reduces the torque peak ($\theta < 75°$). A supplementary suction zone is formed near the slot of the advancing blade 1, which shifts the appearance of negative torque from $\theta = 105°$ in the nominal case to $\theta = 205°$ for the deformable blade. For the hinged (deformable) blade 2, the contraction of the deformable part generates a smaller arm, which advantageously reduces the returning blade drag.

4.3 Effect of expansion amplitude on the turbine performance

The effects of deformation amplitude on the individual and total instantaneous torque coefficient are shown in Figure 7. For the advancing blade1, it can be seen that the amplitude of 0.5 R_1 displays the widest C_m region, which covers the azimuthal angle between $80° < \theta < 300°$. y reducing the

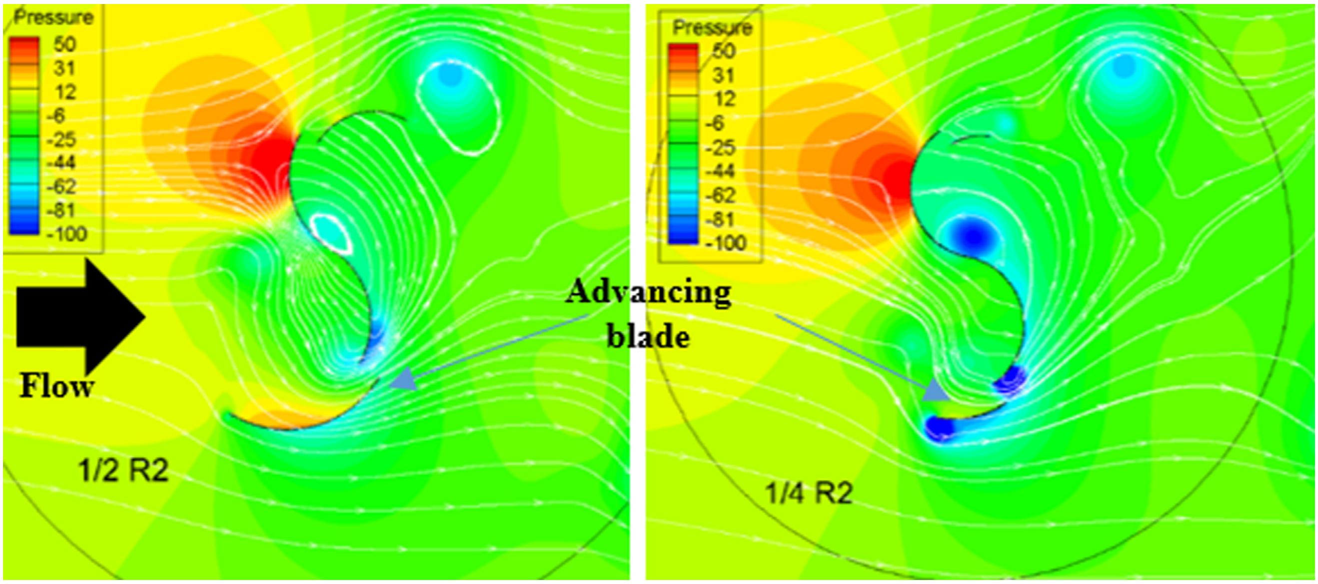

Fig. 10. Comparison of pressure contours.

amplitude from 0.5 R_1 to 0.125 R_1, the C_m of blade1 converges to that of the nominal blade. For the returning blade 2, it can be seen that the deformation is beneficial in the first third of the cycle ($\theta < 120°$). For $120° < \theta < 250°$), the returning rigid blade performs better than all deformable blades. This is attributed to the energy loss due to the blade expansion. For θ >250° higher torque is provided by all deformable blades due to the larger blade arm. From Figures 7c and 7d, the maximum C_m of 0.341 is reached for a blade with the amplitude of 0.5 R_1, which is about 32% times that of a rigid blade.

By looking at the time-mean torque coefficient shown in Figures 7c and 7d, a decrease of 7.85% C_m, as compared to the rigid blade, is noted with an amplitude of 0.125 R_1. As stated previously, the flow control mechanism is associated with the extension and/or the increase in strength of the suction zone along the advancing blade. The appearance of slot breaks down this suction zone, which affect negatively the performance at low deformation amplitudes.

Figures 8a and 8b displays the effect of deformation amplitude on the average torque and Power coefficients. It can be seen that at TSR = 0.4 the flow control using the present technique is not beneficial. At low TSR, The appearance of slot breakdown the suction zone. This helpful zone cannot be retrieved even by using a higher deformation amplitude. For TSR = 1, when the amplitude surpasses 0.25 R_1, the partially deformable blade performs almost better than a rigid blade.

4.4 Effect of deformable part length

This section studied the effect of two arc lengths L = 1/4 R_2 and L = 1/2 R_2 where R_2 is the bucket circular arc length. Figures 9 shows the effect of deformable part length on the instantaneous torque coefficient for A = 0.375 R_1 at TSR = 1. From the previous discussion on how the appearance of slot breakdown the suction zone, it was expected that, the blade with a smaller arc length L = 1/4 R_2 provide higher C_m. Because in this case, the turbine will benefit from a longer arm without disturbing the suction zone. The impact of slot location on the flow structure can be also obtained from the pressure contour plots in Figures 10. It can be noted that another suction zone is formed near the slot of the advancing blade for both cases. However, in the case L = 1/4 R_2, the suction zone is more intense and does not affect the trailing edge vortex. This behavior increases the gain of improvement from 13.2% in the case of L = 1/2 R_2 to 18.9% in the case of L = 1/4 R_2.

5 Conclusion

In this study, a Two-dimensional (2D) numerical model of a deformable Savonius turbine is approved. Partially deformable blades are used to enhance the turbine performance. The Bucket has a time-varying form that changes continuously during the turbine rotation. The trailing edge of the blades expands or contracts relative to the turbine's azimuthal position. An active slot is created, which affects the blade pressure distribution.

The main conclusions can be listed as:

- The flow control mechanism is associated with the extension and/or the increase in strength of the suction zone along the advancing blade.
- The blade with a smaller expandable arc length L = 1/4 R_2 provides higher C_m
- The maximum C_m of 0.341 is reached for a blade with an amplitude of 0.5 R_1, which is about 32% times that of a rigid blade.
- The time-mean torque coefficient shows, a decrease of 7.85% C_m, as compared to rigid blade, for an amplitude of 0.125 R_1.

References

1. E. Antar, M. Elkhoury, Parametric sizing optimization process of a casing for a Savonius vertical axis wind turbine, Renew. Energy **136**, 127–138 (2019)
2. B. Arfaoui, M.T. Bouzaher, B. Guerira, C. Bensaci, On the performance of swing arm flapping turbines, ASME J. Sol. Energy Eng. **143**, 011013 (2020)
3. A. Zereg, N. Lebaal, M. Aksas, Derradji, CFD analysis of a vertical axis wind turbine, in: *Mathematical Modelling of Fluid Dynamics and Nanofluids*,CRC Press, 2024, pp. 184–196
4. F. Wenehenubun, A. Saputra, H. Sutanto, An experimental study on the performance of Savonius wind turbines related with the number of blades, Energy Procedia **68**, 297–314 (2015)
5. F. Guo, B. turbine caused by rear deflector, Energy **196**, 117132 (2020)
6. G. Kailash, T.I. Eldho, S.V. Prabhu, Performance study of modified Savonius water turbine with two deflector plates, Int. J. Rotating Mach. **201**, 516–523 (2012)
7. Y. Triyogi, S. Gunawan, N.A. Fatowil, C.W. Adi, Improving the performance of Savonius wind turbine by installation of a circular cylinder upstream of returning turbine blade, Alex. Eng. J. **59**, 4923–4932 (2020)
8. H. Alizadeh, M.H. Jahangir, R. Ghasempour, CFD-based improvement of Savonius type hydrokinetic turbine using optimized barrier at the low-speed flows, Ocean Eng. **202**, 107178 (2020)
9. M.H. Mohamed, F. Alqurashi, A. Ramadan, D. Thévenin, Enhancement attempts for a three-bladed Savonius turbine performance, Front. Energy Res. **10**, 797–868 (2022)
10. T.B. Mohamed, G. Belhi, Computational investigation on the influence of expandable blades on the performance of a Savonius wind turbine, J. Sol. Energy Eng. **144**, 061003–1 (2022)
11. M.T. Bouzaher, B. Guerira, Impact of flexible blades on the performance of Savonius wind turbine, Arab. J. Sci. Eng. **47**, 15365–15377 (2022)
12. T.B. Mohamed, Effect of flexible blades on the Savonius wind turbine performance, J. Braz. Soc. Mech. Sci. Eng. **44**, 60 (2022)
13. M.V. Driagoi, D.B. Vrinceanu, V.M. Stamate, N.F. Cofaru, Vertical wind turbine with self-limitation system of speed, IOP Conf. Series Mater. Sci. Eng. **399**, 012015 (2018)
14. R. Hassanzadeh, O. bin Yaakob, M.M. Taheri, M. Hosseinzadeh, Y.M. Ahmed, An innovative configuration for new marine current turbine, Energy. **120**, 413–422 (2018)
15. S. Krzysztof, O. Damian, R. Piotr, M. Emil, Numerical investigations of the Savonius, Turbine. Deform. Blades Energ. **13**, 3717 (2020)
16. Bo. Yang, C. Lawn, Fluid dynamic performance of a vertical axis turbine for tidal currents renew, Energy **36**, 3355–3366 (2011)
17. D.D.D.P. Tjahjana, Z. Arifin, S. Suyitno, W.E. Juwana, A.R. Prabowo, C. Harsito, Experimental study of the effect of slotted blades on the Savonius wind turbine performance, Theor. Appl. Mech. Lett. **11**, 100249 (2021)
18. E. Fatahian, F. Ismail, M.H.H. Ishak, W.S. Chang, Aerodynamic performance improvement of Savonius wind turbine through a passive flow control method using grooved surfaces on a deflector, Ocean Eng. **284**, 115282 (2023)
19. A.F. Kaya, A. Acir, E. Kaya, Numerical investigation of wind-lens combinations for improving aerodynamic performance of an elliptical-bladed Savonius wind turbine, J. Braz. Soc. Mech. Sci. Eng. **45**, 309 (2023)
20. J. Priyadumkol, K. Khaothong, W. Chaiworapuek, Experimental investigation of modified Savonius wind turbines, in: I*OP Conference Series: Materials Science and Engineering*, IOP Publishing, 2019, Vol. **501**, No. 1, p. 012054
21. A.L. Manganhar, A.H. Rajpar, M.R. Luhur, S.R. Samo, M. Manganhar, Performance analysis of a Savonius vertical axis wind turbine integrated with wind accelerating and guiding rotor house, Renew. Energy **136**, 512–520 (2019)
22. H. Mohamed, A. Faris, T. Dominique, Performance enhancement of a Savonius turbine under effect of front alguiding plates, Energy Rep. **7**, 6069–6076 (2021)
23. E. Kerikous, D. Thévenin, Optimal shape of thick blades for ahydraulic savonius turbine, Renew. Energy **134**, 629–638 (2019)
24. G. Ferrari, D. Federici, P. Schito, F. Inzoli, R. Mereu, CFD study of Savonius wind turbine: 3D model validation and parametric analysis, Renew. Energy **105**, 722–734 (2017)
25. K. Kacprzak, K. Sobczak, Computational assessment of the influence of the overlap ratio on the power characteristics of a classical Savonius wind turbine, Open Eng. **5**, 314–322 (2015)
26. T. Wenlong, S. Baowei, H. James, Z. Van, Parakram P computational fluid dynamics prediction of a modified Savonius wind turbine with novel blade shapes energies **8**, 7915–7929 (2015)
27. R.E. Sheldahl, B.F. Blackwell, L.V. Feltz, Wind tunnel performance data for two- and three-bucket Savonius rotors, J. Energy **2**, 160–164 (1978)

Cite this article as: Alaeddine Zereg, Mohamed Taher Bouzaher, Mounir Aksas, Nadhir Lebaal, Performance enhancement of Savonius wind turbine through partially deformable blades, Int. J. Simul. Multidisci. Des. Optim. **15**, 8 (2024)